ISTITUTO NAZIONALE DI FISICA NUCLEARE

Sezione di Lecce

INFN/TC-91/13
13 Dicembre 1991

V. Nassini, C. Padula, A. Pecoraro:

METAL–PHOTO CATHODE ELECTRON SOURCE SWITCHED BY AN XeCl

Servizio Documentazione
dei Laboratori Nazionali di Frascati

INFN - Istituto Nazionale di Fisica Nucleare
Sezione di Lecce

INFN/TC-91/13
13 Dicembre 1991

METAL-PHOTO CATHODE ELECTRON SOURCE SWITCHED BY AN XeCl LASER

V. NASSISI C. PADULA AND A. PECORARO
Department of Physics, University of Lecce
Istituto Nazionale di Fisica Nucleare sez. Lecce
C.P.193 73100 Lecce-I

ABSTRACT

An XeCl excimer laser has been used to produce photoelectrons from a Zn metal target. The electrons produced have been accelerated and picked up by a collector anode. The coaxial structure of the cathode-anode allowed electron beams to be recorded with risetime less than 1 ns. Measurements of the electron intensity and of the evolution time varying the laser intensity and the acceleration voltage have been made and the space-charge limited and the emission limited flow conditions have been determined. The maximum current density achieved was 6.7 A/cm^2 and a charge of 6.8 nC per pulse was delivered. The experimental conditions in order to obtain current beams having a duration time like that of the pulse laser have been found.

1. INTRODUCTION

The new accelerator machines as well as the pulsed x-ray sources need electron bunches of high current density within very short duration time[1,2]. Intense electron sources of fast risetime are difficult to construct. Thermionic emission, mechanism used for this end, generates electron beams but their duration time is longer than that of the electric field applied and can cause surface damage. Besides, this method decreases the brightness, B, of photoemitted electrons which is calculated by the expression

$$B = \frac{J\,\varepsilon}{\pi\,k\,T} \qquad (1)$$

where J is the photoemitted current density, ε is the longitudinal energy and T is the temperature.

In the last years photocathodes have been used as electron sources for the production of spin-polarized electrons[3,4]. metallic photocathodes present a longer life, work at modest vacuum, are cheap and can present a fast rise time as that of driving laser. The work function of the metals is higher than 3.5 eV which is near to excimer laser photons energy. In fact, this last energy falls in the range from 3 to 6 eV.

Recently KrF excimer lasers which generate photons of 5 eV (248 nm), on metallic target of Cu, Al [5] and Au [6] have been used. The measured photoemission quantum efficiencies are about 10^{-5} which are sufficient to make photodiodes having current up to tens A/cm^2.

In this work a XeCl excimer laser generating photons of 4.03 eV (308 nm) described in the next section, and a vacuum chamber containing a Zn target and a coaxial collector have been used. The coaxial collector system allowed to apply the accelerating voltage and to measure the electron beam current.

The photoemission effect depends on the surface photo effect, volume photo effect and thermionic electron emission. For high

electric field applied the Schottky effect is present which reduces the work function of target used.

The lowering of the work function increases the electron current but can increase the duration time due to the thermionic emission effect.

The electron beam current and the photodiode pulse waveforms were recorded by a fast digitizing oscilloscope (Gould 400 MS/s). The fast photodiode used was a ITT F4115. A joulemeter ED 200 were used to measure the incident laser energy.

2. EXPERIMENTAL APPARATUS.

In this experiment, we have build a new excimer laser having a very compact discharge and preionization electric circuit.

The electrodes are contained in a PVC tube together with the discharge capacitors and the preionization system. The preionization system is formed by 40 small commercially preionization spark gaps (Nippon Dense Japan) fixed very near to an electrode in order to illuminate the whole laser gas. The electric circuit is of capacitor charge transfer type. A spark gap allows to the internal capacitor to charge at the voltage provided by the external capacitor. During the discharge phase, the internal capacitors transfers their stored energy into the laser mixture without to across the preionization spark gaps. This system limited the discharge impedance during the discharge phase.

Two quartz windows tilted at 5^{o} to the optical axis seal the laser chamber. This configuration allows to apply unstable cavity to laser chamber.

The laser beam was lead into a vacuum chamber by a 45^{o} tilted mirror (M) and by a 50 cm focal length lens (L) which converges the laser beam on the target, Fig. 1. In this way the laser beam can be more easily centered on the target. Besides, changing the lens position, it is possible to vary the incident laser fluence

on the target.

The electron chamber is made of stainless steel and is shown in Fig. 1. At one end of the chamber is applied a quartz window, W, which allows to the laser beam to go into, while the other end contains the cathode and the electron accelerator. The distance cathode-anode was fixed at 3 mm. The cathode is charged at high voltage up to 3 kV and is connected to ground by four buffer capacitors of 1nF , 15 kV. The anode is formed by a stainless steel grid with 4 meshes per mm^2. The optical transmission is about 64%. The grid structure (C) is coaxial with the chamber to prevent noises.

The calibration of the collector was accomplished by a current generator and a fast voltage divider (D). Fig. 2 shows the testing fixture with the voltage divider mounted on the chamber in order to record the voltage of the current pulse. During this calibration the buffer capacitors were shorted. Fig. 3. shows the input pulse and the collector response. From this result we can see that the output pulse fits the input pulse within a 5% tolerance.

During the experiment the laser chamber was filled with a 0.1 % HCl, 1.7 % Xe, 1.9 % He and 96.3 % Ne at a total pressure of 300 kPa. The maximum output laser energy was 100 mJ and 13 ns long. Lower energy values were achieved by inserting neutral density filters on optical axis near the lens L. The vacuum chamber was pumped out up 10^{-5} Torr and the current was measured after a hundred shots in order to clean the target surface.

For the laser intensity range used and for the low repetion rate of the laser, pure photoelectric signal, indisturbed by thermionic emission, have been obtained.

3. RESULTS AND DISCUSSION.

Using the 4.03 eV photon energy of the excimer laser and the 3.7 eV work function of zinc, we have done experiments fixing the distance between the lens L and the cathode which determined the

laser spot on the target.

Figs. 4, 5 and 6 show the peak values of the current as a function of the electric field applied and with 23, 15 and 4.5 mJ of incident laser energy, respectively. During these experiments the lens was fixed at 30 and 38 cm from the cathode forming a laser spot on the target of about 0.5 and 0.06 cm^2. From Fig. 4, (23 mJ) one can see that the output current provided by the the 0.5 cm^2 laser spot is higher than that provided by the 0.06 cm^2 laser spot. This behavior can depend by the different current density which determines different space-charge limited values. In fact the current flow provided by 0.5 cm^2 laser spot was space-charge limited up to 0.83 MV/m, while the current flow provided by 0.06 cm^2 laser spot was space-charge limited at values larger than 1 MV/m. When a lower incident laser energy was used the behavior described above is much more evident. In fact, from Fig. 5, (15 mJ) at low electric field, the output current provided by 0.5 cm^2 laser spot is larger than that provided by 0.06 cm^2 laser spot and became lower for high electric field. In this case the space-charge limited values were up to 0.5 and 0.33 MV/m for 0.5 and 0.06 cm^2 laser spots, respectively. Finally, at very low laser energy (4.5 mJ) one can note that the output current provided by 0.06 cm^2 laser spots, Fig. 6, is larger than that provided by the 0.5 cm^2 laser spot and can easily suppose that the space-charge limited values were lower than 0.2 MV/m.

Besides, because new electron machines as well as pulsed X-ray sources need electron bunches of short duration time , we have also done measurements of the duration time of the current pulse. This duration time (FWHM) was compared with that of the laser pulse (FWHM). Figs. 7,8 and 9 report the experiment results of the current lengthening determined as difference between the current duration time and the laser duration time with the incident laser energy of 23, 15 and 4.5 mJ, respectively and with a laser spot of 0.5 and 0.06 cm^2.

We can observe that the current pulse duration is longer at small electric field applied and achieves an almost constant value at high electric field values. Besides, these time values

are higher at high incident laser energy values which provides a higher output current density and then a higher space-charge limited value. When the 15 mJ laser energy was used the current lengthening behavior changed as laser spot changed and it became lower for 0.06 cm^2 laser spot at high electric field applied. This last behavior can be due to higher space-charge limited value for 0.06 cm^2 laser spot than that for 0.5 cm^2 laser spot at the same incident energy. In fact, for 4.5 mJ of laser energy the current lengthening is shorter than that obtained from 15 mJ laser energy, and this can be only ascribed to the low space- charge limited value.

Fig. 10 shows the evolution time of the current and of the laser with the lens fixed at 38 cm, with an electric field of 0.33 MV/m and with 23 mJ incident laser energy. We can see that peak of the current is delayed of about 3 ns from laser peak due to the high space-charge density achieved. Current pulses of the same duration time of the laser were obtained at low laser energies and with a consistent electric field applied. In fact, from Fig. 8 for 4.5 mJ laser energy and with an electric field higher than 0.33 MV/m, the current lengthening is only 0.5 ns longer than that of the laser pulse. This lengthening is comparable to the experimental errors.

4. CONCLUSIONS.

Measurements of the current flow generated by an XeCl excimer laser on a Zn target were made. An output electron current with an duration time of about that of the laser beam were obtained. The maximum current density achieved was 6.7 A/cm^2 but with a current pulse longer than that of the laser.

Besides, in this work for first time the XeCl laser was used for production of electrons. It delivered a charge of 6.8 nC per pulse at maximum incident energy and electric field applied.

REFERENCES

[1] C.H. Lee, P.E. Oettinger, E.R. Pugh, R. Klinkowstein, J.H. Jacob, J.S. Fraser and R.L. Sheffield. IEEE Trans. Nucl. Sci. NS.32, 3045 (1985)

[2] Y. Kawamura, K. Toyoda and Kawai, Appl. Phys. Lett. 45, 307 (1984)

[3] D.T. Pierce, R.G. Celotta, G.C. Wang, W.N. Unertl, A.Galens, C.E. Kuyatt and S.R. Mielczareck, Rev. Sci. Instrum. 51, 478 (1980)

[4] G. Farkas, Z.G. Horvat, C. Toth, C. Fotakis, and E. Hontzopoulos, J. Appl. Phys. 62, 4545 (1987)

[5] S.W. Downey, L.A. Builta and D.C. Moir, Appl. Phys. Lett. 49, 911 (1986)

[6] D. Charalambidis, E. Hontzopoulos, C. Fotakis, G. Farkas and C. Toth, J. Appl. Phys. 65, 2843 (1989)

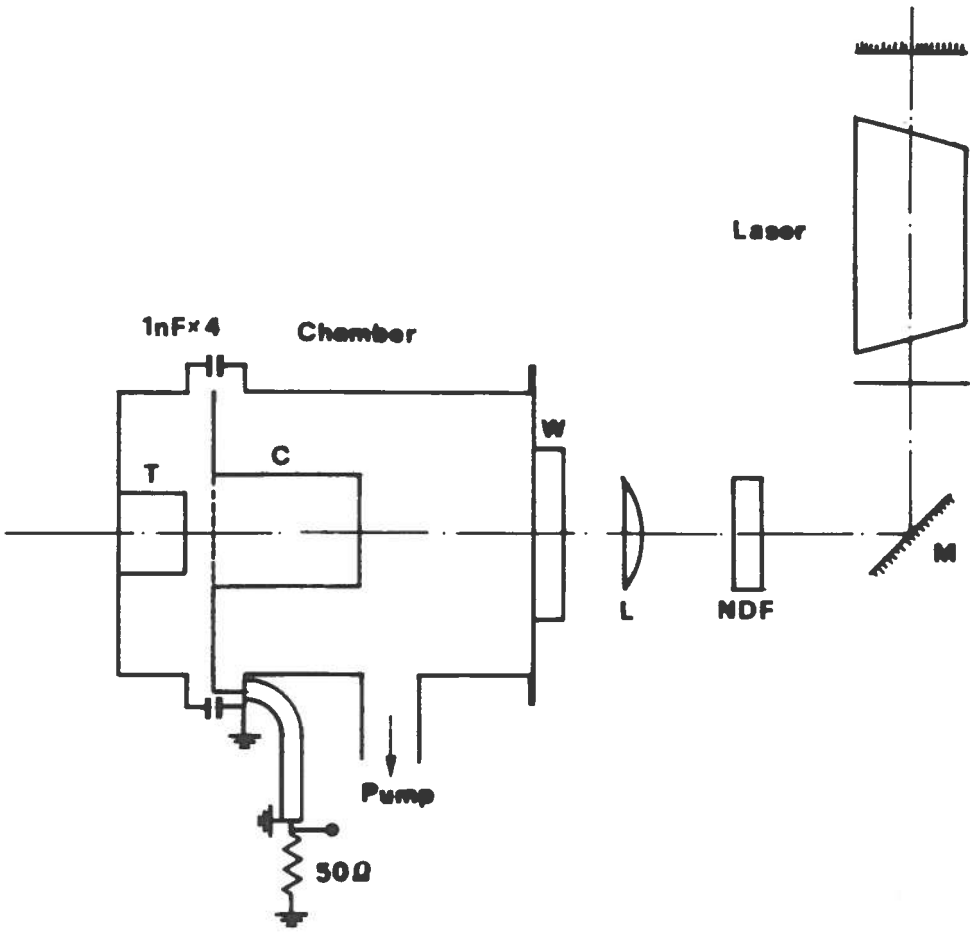

Fig. 1: schematic diagram of the experimental set up used. T: cathode or target, C: collector or anode, L: lens, W: window, NDF: neutral density filter.

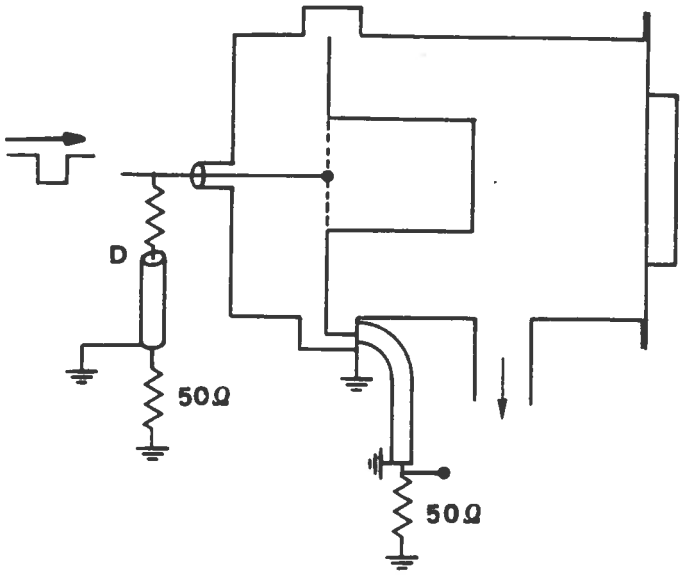

Fig. 2: schematic diagram of the coaxial calibration fixture showing the input pulse and the voltage divisor D.

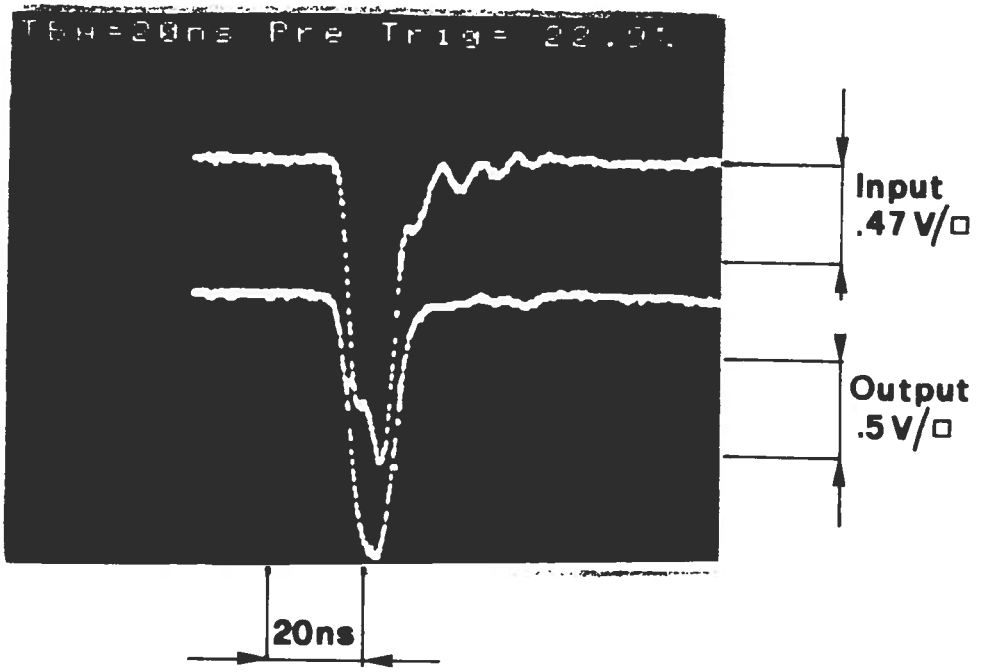

Fig. 3: waveforms of the input pulse (upper trace) and of the response (bottom trace)

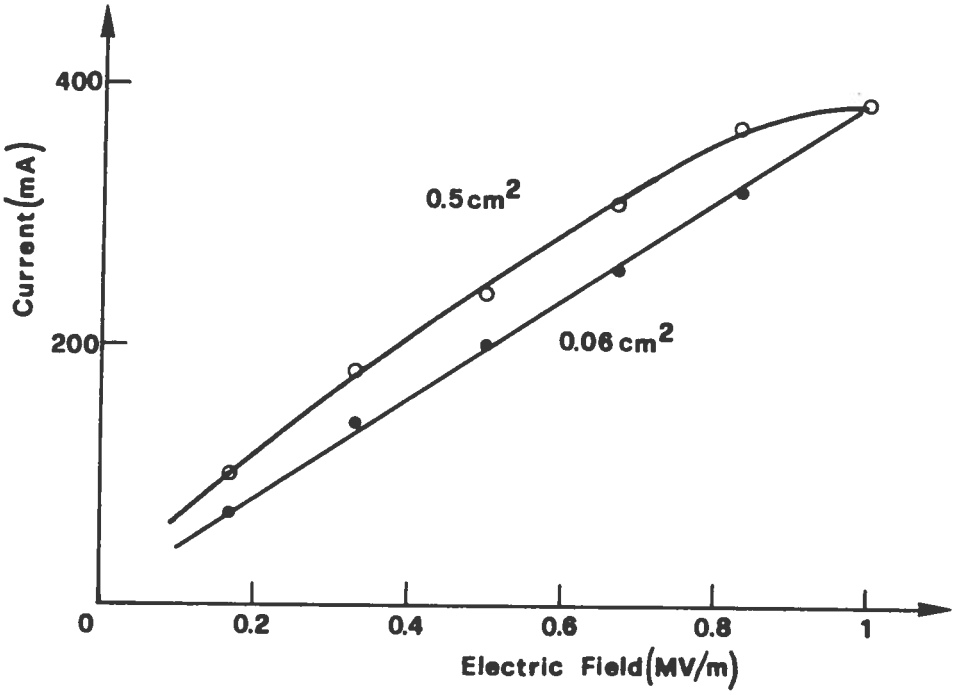

Fig. 4: output current as a function of the electric field applied with 23 mJ icident laser energy.

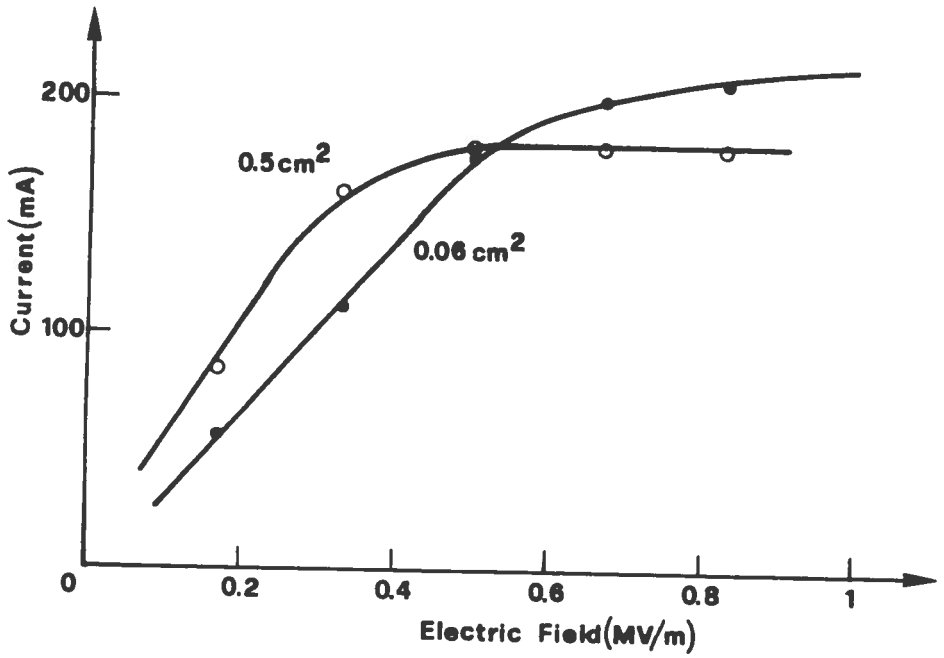

Fig. 5: output current as a function of the electric field applied with 15 mJ incident laser energy.

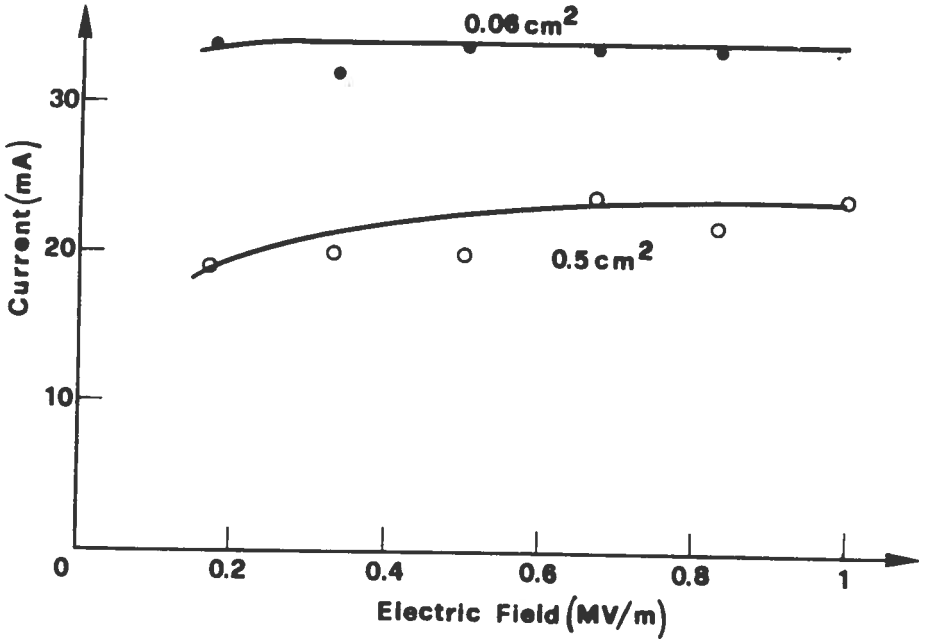

Fig. 6: output current as a function of the electric field applied with 4.5 mJ incident laser energy.

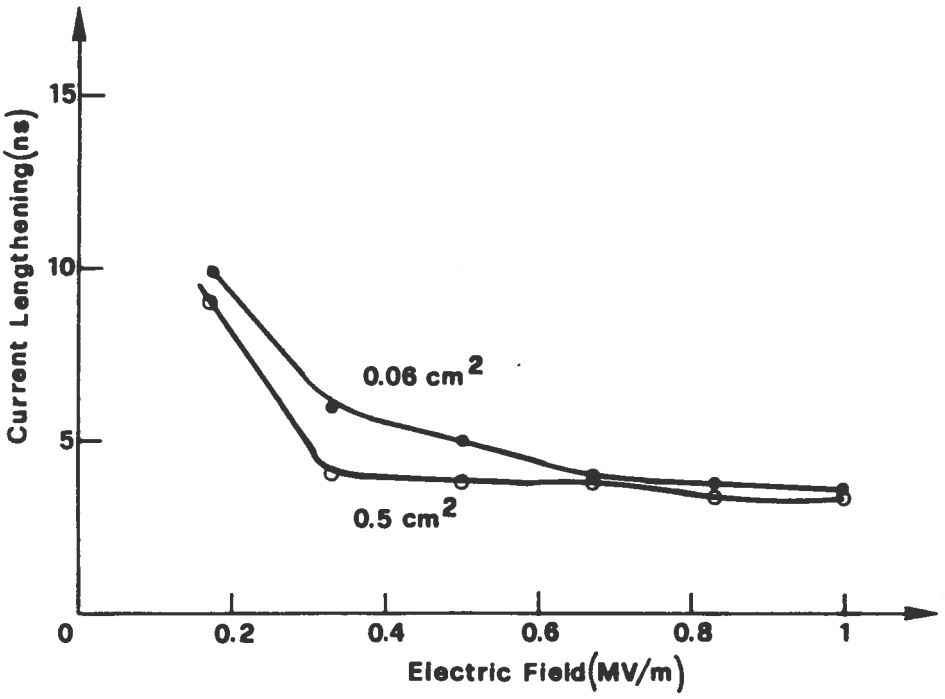

Fig. 7: current lengthening as a function of the electric field applied with 23 mJ incident laser energy.

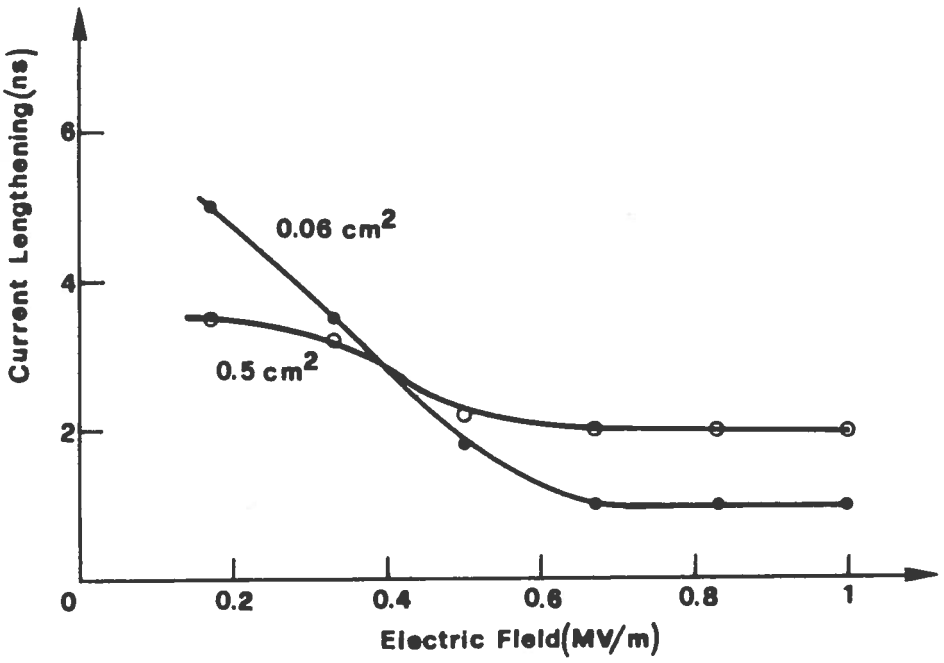

Fig. 8: current lengthening as a function of the electric field applied with 15 mJ incident laser energy.

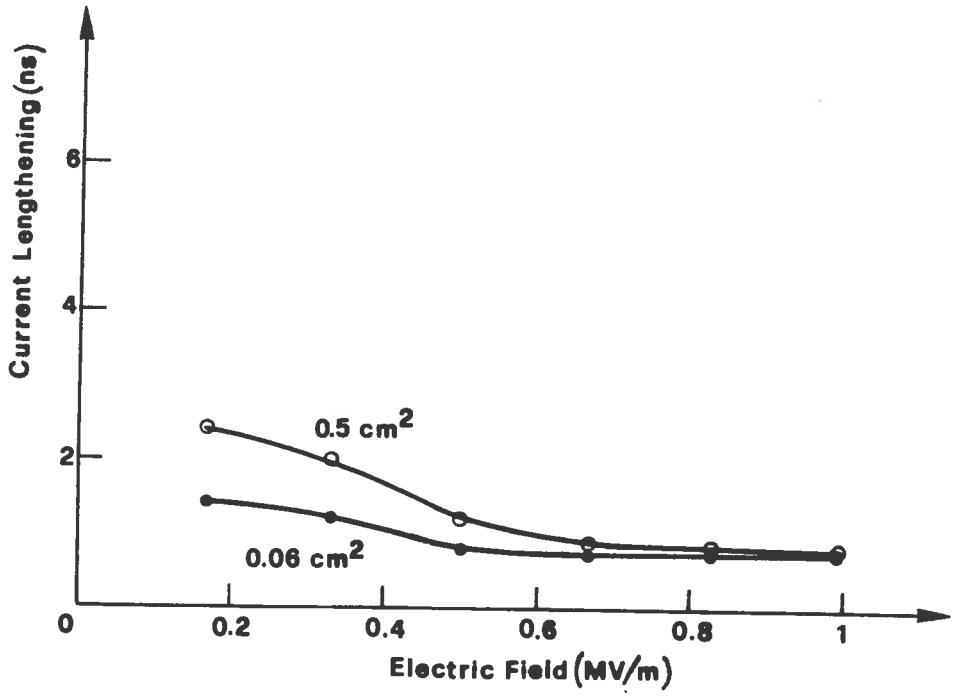

Fig. 9: current lengthening as a function of the electric field applied with 4.5 mJ incident laser energy.

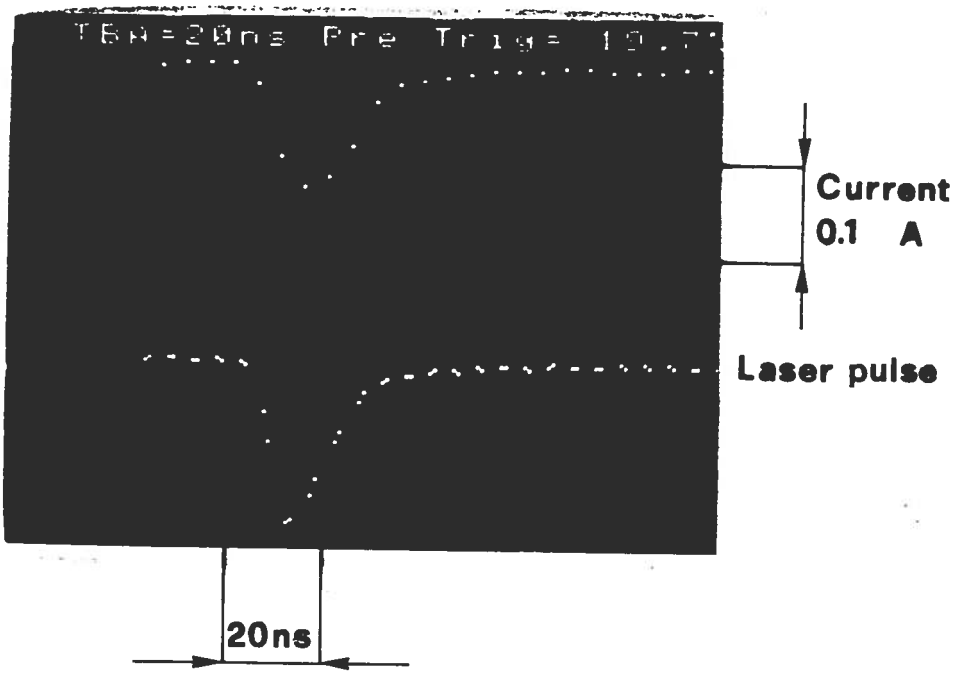

Fig. 10: waveforms of the output current (upper trace) and of the laser pulse (bottom trace) recorded with the lens at 38 cm from the cathode and at 23 mJ laser energy.